Research Article | Vol. 28, No. 17 / 17 August 2020 / Optics Express 25400
Optics EXPRESS

Ultra-low phase noise microwave generation with a free-running monolithic femtosecond laser

MANOJ KALUBOVILAGE,[1] MAMORU ENDO,[1] AND THOMAS R. SCHIBLI[1,2,*]

[1]Department of Physics, University of Colorado, Boulder, CO 80309-0390, USA
[2]JILA and NIST, University of Colorado, Boulder, CO 80309-0440, USA
*trs@colorado.edu

Abstract: Phase noise performance of photonic microwave systems, such as optical frequency division (OFD), can surpass state-of-the-art electronic oscillators by several orders of magnitude. However, high-finesse cavities and active stabilization requirements in OFD systems make them complicated and potentially unfit for field deployment. Ultra-low noise mode-locked monolithic lasers offer a viable alternative for a compact and simple photonic microwave system. Here we present a free-running monolithic laser-based 8 GHz microwave generation with ultra-low phase noise performance comparable to laboratory OFD systems. The measured noise performance reached −130 dBc/Hz at 100 Hz, – 150 dBc/Hz at 1 kHz, and –167 dBc/Hz at 10 kHz offsets from the 8-GHz carrier. We also report a sub-Poissonian noise floor of −179 dBc/Hz above 30 kHz (timing noise floor of 32 zs $Hz^{-1/2}$), which is ∼12 dB below the noise floor of time-invariant shot noise. In addition to the low phase noise, the system is compact, with a power consumption of less than 9 W, and offers excellent potential for mobile or space-borne applications.

1. Introduction

Ultra-low phase noise X-band (8-12 GHz) microwaves are of great interest due to their growing demand in many fields such as high-performance radar systems [1], communication [2], time-frequency metrology [3], and signal measurement instrumentation [4]. The recent attraction towards mobile, airborne, and space applications of ultra-low noise X-band microwaves requires microwave oscillators that offer smaller size, weight, and power consumption (SWaP). Conventional mobile high-performance X-band oscillators rely on electronic resonators such as sapphire loaded cavities (SLCs), which serve as a frequency discriminator (FD) to achieve low phase noise performance [5]. However, the relatively modest quality factor (Q-factor) of room-temperature SLCs and other technical limitations, such as carrier signal reflection, limit the achievable microwave spectral purity of these oscillators [6]. Several photonics-based approaches have addressed some of these limitations with ultra-low noise performance with wide tunability [7–14]. The optical frequency comb (OFC)-based phase-coherent optical frequency division (OFD) scheme has demonstrated a superior phase noise performance compared to other methods with zeptosecond-level timing noise [15].

OFD-based microwaves are achieved via photo-detecting of an ultra-stable optical pulse train from an OFC, which transfers the stability from the optical to the microwave domain [14–16]. Current commercial OFCs are compact and robust. The free-running intrinsic noise of these OFCs, however, is not sufficiently low for microwave generation, and therefore, require external stabilization of the repetition rate f_{rep} and the carrier-envelope offset frequency f_{ceo} with wide feedback bandwidth. The f_{rep} of an OFC is stabilized by tightly locking one of the comb modes to an ultra-stable optical reference, which is commonly derived from a continuous wave (CW) laser actively locked to an ultra-low expansion (ULE) Fabry-Pérot (FP) cavity in a vacuum. The

#399425 https://doi.org/10.1364/OE.399425
Journal © 2020 Received 9 Jun 2020; revised 31 Jul 2020; accepted 2 Aug 2020; published 12 Aug 2020

Optics EXPRESS

f_{ceo} stabilization is achieved via an f-2f interferometer, which requires an octave-spanning optical spectrum. Such broad spectra are typically obtained via supercontinuum generation, which often requires pulse amplification [17]. The optical cavity and supercontinuum generation requirements dramatically increase the SWaP and the complexity of the system, making traditional OFDs less desirable for mobile applications.

In this paper, we demonstrate a novel approach to X-Band photonic microwave generation using a free-running, quantum noise-limited, monolithic mode-locked laser (MMLL) [18,19]. The proposed method entirely rely on the ultra-low intrinsic noise of the MMLL and does not require any f_{ceo} or f_{rep} stabilization. This significantly reduces the complexity and the SWaP of the system compared to a traditional OFD scheme. With this approach, we demonstrate a phase noise performance of -130 dBc/Hz at 100 Hz offset, -150 dBc/Hz at 1 kHz offset and -167 dBc/Hz at 10 kHz offset for an 8 GHz carrier with thermal noise limited sub-Poissonian shot noise floor of −179 dBc/Hz above 30 kHz (Johnson-noise-limited timing noise floor of ~32 zs $Hz^{-1/2}$, measured in the microwave domain at 8 GHz). The phase noise performance of this system surpasses the similar earlier attempts of using a free-running fiber-based OFC for ultra-low noise microwave generation by more than 23 dB at 10 kHz offset for an 8 GHz carrier [3,20]. Compared to the recently demonstrated free-running OFC transfer oscillator based microwave generation approach, this system is better than ~20 dB at 10 kHz offset, scaled to an 8 GHz carrier [12]. Furthermore, this free-running MMLL based system outperforms the current soliton microcomb approaches by more than 50 dB [9]. The phase noise performance reported here is comparable to state of the art OFDs, but with smaller physical footprint and about an order of magnitude lower power consumption.

2. Experimental setup

Figure 1 (top) shows a schematic of the microwave generation setup. It consists of a free-running 1-GHz MMLL as the quantum-noise limited optical oscillator, an erbium-doped fiber amplifier (EDFA) for optical pulse amplification, an acousto-optic modulator (AOM) to suppress the relative intensity noise (RIN), a three-stage pulse interleaver for repetition rate multiplication and a modified uni-traveling carrier photodiode (MUTC) for microwave generation [21].

The MMLL laser is built from a low-loss CaF_2 spacer combined with an Er:Yb:glass gain medium and a semiconductor saturable absorber mirror (SESAM) to initiate and maintain mode-locking [18]. CaF_2 offers excellent transparency and near-zero second-order dispersion at 1550 nm, which is important for low-noise operation. The third-order dispersion is compensated through a Gires-Tournois interferometer (GTI) coating, which is directly deposited onto the CaF_2 spacer. The SESAM, which initiates and maintains the mode-locked operation, is an InGaAs quantum-well grown on an AlGaAs/GaAs Bragg stack. The laser output is a 1-GHz $sech^2$-shaped pulse train with a pulse duration of ~150 fs at a center wavelength of 1557 nm [18]. The simulated free-running performance of this monolithic laser is –160 dBc/Hz at 1 kHz, –191 dBc/Hz at 10 kHz and –213 dBc/Hz at 100 kHz offset frequencies at the 1 GHz repetition frequency [19]. The optical power output of the MMLL is 35 mW. Approximately 2% of the light from the MMLL is diverted to an InGaAs PIN photodiode (PD, Hamamatsu, G12180-003A) for measuring and suppressing the relative intensity noise (RIN) of the MMLL.

The EDFA amplifies the rest of the output of the MMLL to 50 mW. The amplified 1 GHz optical pulse train then traverses a three-stage optical pulse interleaver based on polarization beam splitters (PBSs) and quarter-wave plates (QWPs) to obtain the desired 8 GHz pulse repetition rate. The repetition rate multiplication reduces the peak optical power of the pulses and concentrates the power in the desired harmonic (8 GHz), which reduces the saturation effects in the MUTC [22,23]. However, a small timing delay error in the pulse interleaver can significantly increase the phase noise floor of the microwave [24]. In the experiment, each interleaving stage is carefully

Optics EXPRESS

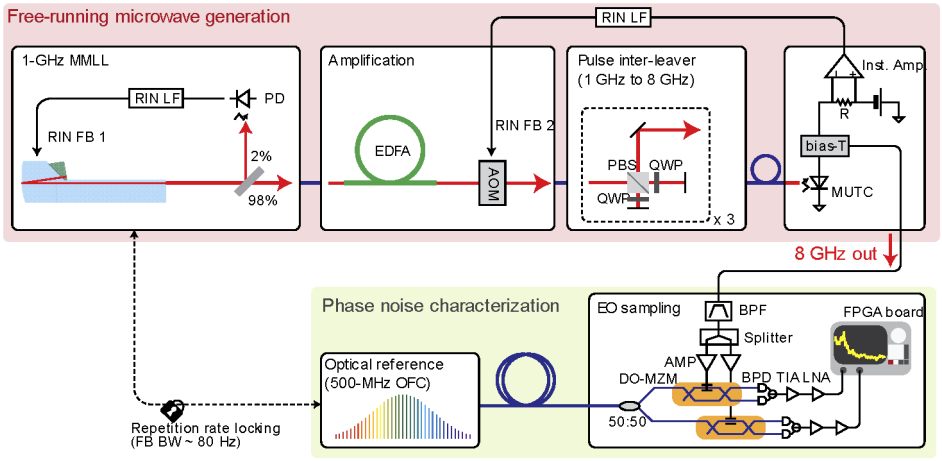

Fig. 1. Schematic of the microwave generation and characterization setup. The top part of the setup shows the microwave generation using a free-running mode-locked monolithic laser. The phase noise is measured using Mach-Zehnder modulator-based electro-optics (EO) sampling technique (bottom part). The pulse repetition rate of the MMLL is stabilized to the optical reference using a slow feedback bandwidth (FB BW) loop. The optical reference is a cavity stabilized 500-MHz optical frequency comb (see methods). MMLL: mode-locked monolithic laser, PD: photodiode, OFC: optical frequency comb, LF: loop filter, AOM: acousto-optic modulator, EDFA: erbium-doped fiber amplifier, PBS: polarization beam splitter, QWP: quarter-wave plate, Inst. Amp.: instrumentation amplifier, R: shunt resistor, Bias-T: bias tee, BPF: bandpass filter, MUTC: modified uni-traveling carrier photodiode, BPD: balanced photodetector, TIA: transimpedance amplifier, LNA: low noise amplifier, DO-MZM: dual-output Mach-Zehnder modulator, AMP: RF amplifier, FPGA: field programmable gate array.

tuned to minimize the timing delay errors and to achieve +2 dBm microwave power at 8 GHz carrier at the output of the bias tee.

The RIN on the microwave signal is directly measured via a 5 Ohm shunt resistor (R) placed in series with the bias voltage supply of the MUTC detector and is monitored with an instrumentation amplifier (Inst. Amp.) with a gain bandwidth of ~1 MHz. A proportional controller is used to suppress this RIN using an AOM operating in zero-order mode and driven by an amplitude modulated 80 MHz carrier to effectively produce a voltage-controlled optical attenuator. This AOM is placed before the optical pulse interleaver, as shown in Fig. 1, top. This RIN feedback loop has an effective bandwidth of ~350 kHz and yields more than 10 dB of RIN suppression below 100 kHz. The MUTC is operated at 6 V reverse bias to minimize the amplitude to phase noise conversion (AM-PM conversion), which originates primarily from the increased response time caused by space charge effects in the detector [25,26]. The AM-PM conversion factor was measured by adding an AM tone on the optical pulse-train and was found to be about -58 dB at the 8 GHz carrier, said bias voltage, and for a 7 mA photocurrent. The total power consumption of this microwave generation scheme is less than 9 W (2 W for MMLL, 2 W for EDFA, 2 W for AOM driver, and < 3 W for RIN servos and MUTC bias), which is about an order of magnitude less than our traditional OFD system (>100 W).

Figure 1 bottom shows our approach to characterize the generated microwaves by a direct electro-optic comparison technique involving two dual-output Mech-Zehnder modulators (DO-MZM, EOSPACE, AX-2 × 2-0S5-10-PFA-PFA), combined with a cross-spectrum technique. A detailed description of this method is given in [27]. In short, the DO-MZMs optically sample the microwave signal against a f_{rep} and f_{ceo} stabilized OFC operating at 500 MHz (1/16th of the

Optics EXPRESS

microwave carrier frequency, see Appendix). The time-averaged cross-spectrum between two channels yields the desired phase-noise data, free of statistically independent instrumentation noise that is typically present in each channel. Latter includes flicker noise of the DO-MZMs, the RF amplifiers, and the baseband diodes, as well as electronic noise from RF and baseband amplifiers, and shot-noise due to the photocurrent on these baseband diodes. An FPGA-based sampling board (modified Red Pitaya STEMLab 125-14) is used to achieve ~30 dB suppression of these statistically independent noise terms within less than 5 minutes of averaging time (4 kHz RBW). The drawback of this homodyne method is that the device-under-test (DUT) must have the same repetition rate (or a harmonic thereof) of the reference OFC. Therefore, during the measurements, the repetition rate of the monolithic laser is matched to the 16^{th} harmonic of the reference OFC with a feedback bandwidth of ~80 Hz. The phase noise data below this loop bandwidth is in-loop, and hence, is not presented here. The reason a homodyne method was chosen here is the large dynamic range of the phase noise power spectrum of >180 dB (from the inverse measurement time to ~1 MHz), which far exceeds the dynamic range of any high-speed sampling board.

3. Results and discussions

Figure 2 summarizes the results of the 8 GHz microwave single-sideband phase noise present around the 8-GHz carrier. Figure 2(a) shows the measured phase noise. Figure 2(b) is the estimated noise performance of the system, calculated by adding the measured flicker noise of the MUTC detector (Fig. 2(c)) and the quantum-noise limited contribution from the free-running MMLL (Fig. 2(d)). Flicker noise of the MUTC for a 2 dBm carrier at 8 GHz is measured using the same dual DO-MZM setup (see Appendix). The noise of the MMLL at low offsets (<3 kHz), is dominated by classical RIN-driven self-steepening effects due to the slow saturable absorber used in the MMLL, which is eliminated by the aforementioned RIN feedback to the MMLL pump. Above 3 kHz, the Gorden-Haus timing jitter is dominant (see [19] and Appendix). The performance of the system above 10 kHz offsets is limited by the flicker noise of the MUTC and the 50 Ohm thermal noise floor (Fig. 2(f)). The measured noise generally agrees well with the calculated performance (see Figs. 2(a) and (b)). The dip in the phase noise measurements around 40 kHz is due to the “cross-spectrum collapse": an artifact of the dual-channel cross-spectrum method, and is typically observed when the oscillator’s noise approaches the thermal noise limit of the 50 Ohm system [28,29]. The source of this effect is the thermal noise originating from the isolation resistor from the Wilkinson splitter (‘Splitter’ in Fig. 1), which appears anti-correlated between the two outputs. The cross-spectrum measures the differential thermal noise between the power splitter and the oscillator, underestimating the true phase noise of the oscillator at the thermal noise floor. It has been shown that the cryogenic cooling of the splitter can reduce this effect [28]. The sharp peaks below 1 kHz and bumps near 2.5 kHz and 20 kHz are related to acoustic noise and RIN servos of the optical reference comb, respectively. The measurement limit inferred from in-loop signals of optical reference is shown in the dashed grey curve (Fig. 2(g)). At offsets above 100 kHz, the phase noise of the system is fully limited by the Johnson noise, and is, therefore, frequency independent.

At sufficiently high photocurrents, the microwave phase noise floor is limited by the shot noise, which arises from the discrete nature of the impinging photons on the photodiode. Generally, shot noise is treated as a Poisson process, and the one-sided power spectral density for a photocurrent I is given by $S_i(f) = 2qI$ where q is the electron charge. In the detection of ultrashort optical pulse trains, however, the photon statistics strongly depend on the optical pulse width and the pulse timing interval, and therefore, cannot be treated as a continuous, statistically independent distribution [30]. These shot noise correlations can be exploited to improve the fundamental shot noise limit by several orders of magnitude [30,31]. For example, for a sech^2-shaped pulse train with a repetition rate f and full width at half maximum (FWHM) pulse duration Δt, it can be

Optics EXPRESS

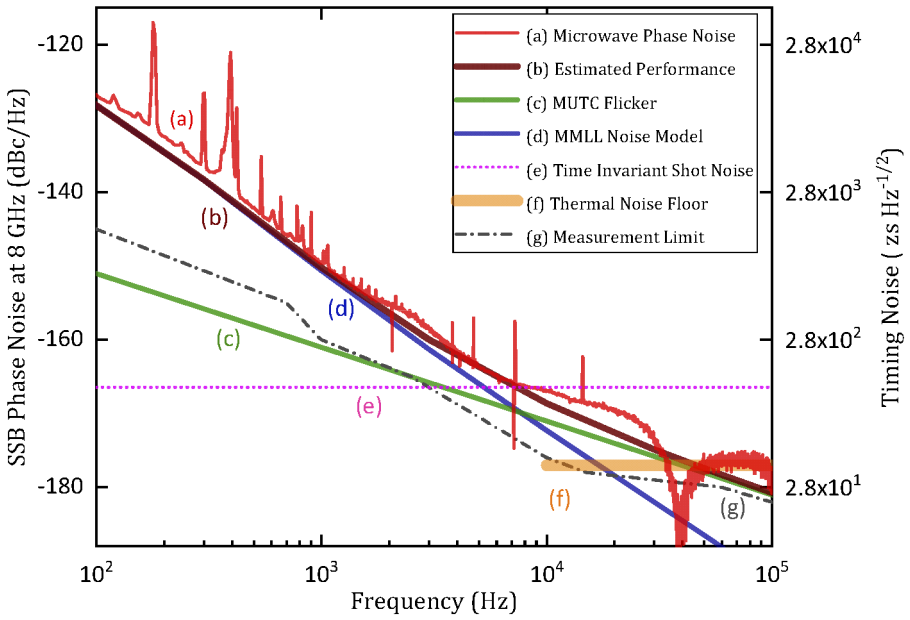

Fig. 2. SSB Phase noise result of MMLL-based microwave generation. (a) Measured phase noise at 8 GHz carrier, (b) Estimated phase noise performance, (c) Measured flicker noise of the MUTC at 8 GHz following dBc/Hz, (d) Modeled quantum noise of the MMLL converted to 8 GHz, (e) Calculated time-invariant shot noise for 7 mA photocurrent (f) Thermal noise floor, corresponds to timing noise of 32 zs $Hz^{-1/2}$, (g) Measurement limit approximated from the in-loop signals from reference comb. The dip in the phase noise measurement at 40 kHz is due to the "cross-spectrum collapse" (see text).

shown that the shot noise limited phase noise floor is improved by a factor β,

$$\beta = [1 - \pi^2 f \tau_s \times \mathrm{csch}(\pi^2 f \tau_s)], \tag{1}$$

where τ_s is the time scaling parameter given by $\Delta t/1.763$. In our measurements, we observe about 12 dB sub-Poissonian shot noise floor improvement, more than 6 dB better than the previously reported value [31]. This Johnson-noise-limited phase noise floor corresponds to the timing noise of 32 zs $Hz^{-1/2}$.

Figure 3 compares the results with our system (a) and several state-of-the-art X-band microwave oscillators scaled to an 8-GHz carrier frequency (b-f) [5,6,14,15]. The light blue curve (d) shows the, to our knowledge, best phase noise reported to date using the OFD scheme with 41 zs $Hz^{-1/2}$ timing noise floor [15]. Laboratory OFD systems (c, d) offer a lower close to carrier phase noise performance due to the high Q factor and temperature stability of ULE FP cavities. However, for higher offsets, the free-running MMLL-based system is comparable to the best laboratory OFD systems, and the noise performance outperforms the very best commercial X-band microwave oscillators [32]. Reduced long term stability of the oscillator due to the non-zero temperature expansion coefficient of the CaF_2 spacer of the MMLL is a disadvantage of the proposed method. This could be overcome by phase locking the MMLL to a commercially available external electrical or optical reference such as a rubidium clock or an iodine-stabilized laser, respectively.

Optics EXPRESS

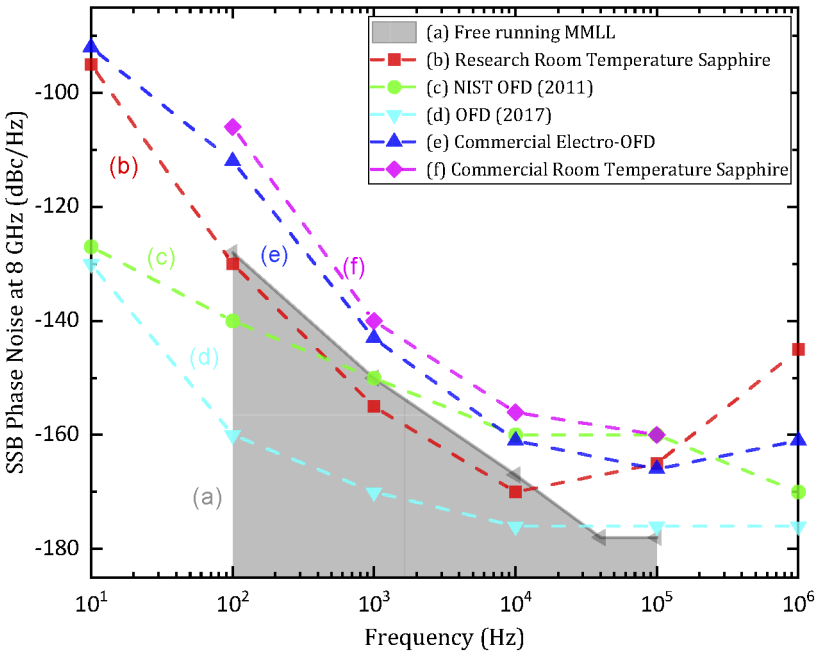

Fig. 3. Approximate single-sideband noise converted to 8 GHz for several state-of-the-art microwave generators. (a) Results of the current work, (b) Research room-temperature sapphire oscillator [6], (c) NIST OFD based photonic generation [14], (d) Current best microwave phase noise results (OFD) [15], (e) Commercial compact electro-optical frequency division based oscillators [8] (see http://hqphotonics.com/), (f) Commercial room temperature sapphire loaded whispering gallery mode oscillator [32] (former Poseidon Instruments).

4. Conclusion

In conclusion, we demonstrate ultra-low phase noise 8-GHz microwave generation with a free-running monolithic mode-locked laser (MMLL). Due to the smaller SWaP of the proposed method compared to the traditional OFD systems, mobile and space microwave applications could greatly benefit from the research reported here. The measured phase noise performance of this approach reaches −130 dBc/Hz at 100 Hz, −150 dBc/Hz at 1 kHz, and −167 dBc/Hz at 10 kHz offsets from the 8-GHz carrier. This noise performance surpasses previously demonstrated free-running laser and soliton microcomb based microwave generation approaches by several orders of magnitude. We also report ~12 dB sub-Poissonian shot noise improvement in ultra-short optical pulse detection. Higher optical powers and MUTCs with high power handling capabilities could further exploit this sub-Poissonian shot noise correlations to improve photonic microwave phase noise floor to unprecedented levels.

Appendix

Phase noise model of free-running MMLL

The most significant sources of the MMLL are Amplified Spontaneous Emission (ASE), Gordon-Haus Jitter (GH), Self-Steepening (SS), and noise due to slow saturable absorber. ASE noise comes from the spontaneous emission from the gain medium, which perturbs the temporal position of the pulse. This ASE noise can also introduce shifts in the center frequency of the laser's optical spectrum, which alters the group velocity of the pulse due to the dispersion of the cavity. This is known as the Gordon-Haus Jitter. The Self-Steepening noise occurs due to Kerr

Optics EXPRESS

effect, which causes a change in the group velocity and couples the amplitude-to-phase noise. In a slow saturable absorber, the front slope of the pulse experience a greater attenuation than the trailing slope. This causes a change in the pulse shape, shifting the center of the pulse in the time domain, which also introduces a phase noise. The relevant phase noise expressions for these noise sources are shown below as single sideband (SSB) spectral density $\mathcal{L}(f)$ [19].

1) Amplified Spontaneous Emission (ASE):

$$\mathcal{L}_{ASE}(f) \approx \frac{0.26\theta g h\nu}{Pf^2}(f_{rep}f_{osc}\tau)^2 \tag{2}$$

where f is the offset frequency away from the carrier f_{osc}, f_{rep} is the pulse repetition rate, P is the average intracavity power, θ is the excess noise factor of the gain, g is the round trip cavity loss, $h\nu$ is the photon energy, and τ is the FWHM pulse duration.

2) Gorden Haus jitter:

$$\mathcal{L}_{GH}(f) \approx L_{ASE} \times \frac{D^2\Gamma_g^2}{g^2 + 9.26\left(\frac{f}{f_{rep}}\right)^2\Gamma_g^4\tau^4} \tag{3}$$

where D is the intra-cavity group delay dispersion and Γ_g is the half width half maximum (HWHM) gain bandwidth.

3) Self Steepening noise:

$$\mathcal{L}_{ss}(f) = \frac{1}{2}\left(\frac{f_{rep}f_{osc}\varphi_{NL}}{\pi f\nu}\right)^2 S_{RIN}(f) \tag{4}$$

where φ_{NL} is the total non linear phase shift for round trip.

4) Slow Saturable Absorber response:

$$\mathcal{L}_{SSA}(f) = \frac{1}{2}\left(\frac{f_{rep}f_{osc}}{f}\ \frac{\partial\Delta t}{\partial s}s\right)^2 S_{RIN}(f) \tag{5}$$

where s is the ratio of the pulse energy over the absorber saturation energy, and Δt is the timing shift arising from the slow response of the absorber.

Optical reference

For the microwave measurements, we use a traditional OFD system as the optical reference. This reference OFD uses a 1550 nm CW laser (NKT photonics, Koheras BASIK MIKRO E15) locked to a high finesse ULE cavity with the finesse of ~400,000 (not shown in Fig. 1) via the Pound-Drever-Hall (PDH) locking scheme. The high finesse cavity is placed inside a temperature-controlled vacuum chamber. In the PDH locking, an additional servo loop is used to the RF input of the electro-optic modulator for further suppressing the residual phase noise of the error signal at high bandwidths, enabling the very low phase noise floor shown as the "measurement limit" in Fig. 2) [33]. The OFC is a homemade solid-state Er-laser with a 500 MHz fundamental pulse repetition rate. A SESAM is used to initiate and maintain mode-locking. The f_{rep} of the laser is tuned by moving mirrors of the laser cavity using piezo modulators. The carrier-envelope offset frequency f_{ceo} of the OFC is locked to an external local oscillator using an f-2f interferometer. The OFC is tightly phase-locked to the cavity-stabilized CW laser using the heterodyne beat between the CW laser and single longitudinal mode of the OFC. The SNR of both beat notes (f_{ceo} and f_{rep}) are about 60 dB at a 100 kHz resolution bandwidth, ultimately enabling a shot-noise limited comb performance resulting in a -197 dBc/Hz noise floor at 8 GHz DUT frequencies.

Optics EXPRESS

Electro-optical sampling

The output from the MUTC is sent through an 8 GHz bandpass filter (BPF, Mini-Circuits, ZBSS-7975-S+) to filter out unwanted harmonics. The filtered 8-GHz signal is then divided into two equal parts using a Wilkinson power splitter (Splitter, Mini-Circuits, ZN2PD-02183-S+). Each section is sent through an isolator, phase shifter, and an 8 GHz amplifier (Custom MMIC, CMD274P4) and then sent into the RF port of each DO-MZM. The DO-MZM is used to sample the microwave signal against the stabilized optical reference described above. About 10 mW of the optical power of the stabilized reference OFC is divided into two using a PM-fiber 50:50 beam splitter and then fed into each DO-MZM, for the microwave-to-optical comparison. The optical output pairs from each DO-MZM are detected using balanced photodiodes (BPD) (about 2 mW of optical power on each diode). The balanced signal is then amplified via transimpedance amplifiers (TIAs), followed by low noise voltage amplifiers (LNAs). The Power spectral density (PSD) of each output is measured using a field programable gate array (FPGA) board with two-channel input (modified Red Pitaya STEMLab 125-14). The time-averaged cross-spectrum between the two channels yields the desired phase-noise data, free of statistically independent instrumentation noise present in each channel [34]. Latter includes flicker noise of the DO-MZMs, RF amplifiers, and the baseband diodes, as well as electronic noise from RF and baseband amplifiers and shot-noise due to the 2 mA of baseband current on each diode. Two separate power supplies are used to minimize common-mode supply noise between two channels. The carrier power of each channel, which measured by unlocking the slow phase lock between optical reference and MMLL, is used to convert the PSD to SSB phase noise. A commercial X-band yttrium iron garnet (YIG) oscillator is used as DUT to further confirm the calibration of the measurement setup by comparing it against a phase noise measurement of a commercial signal analyzer (Keysight, N9030A PXA)

MUTC flicker noise measurement

Flicker noise of the MUTC for a 2 dBm carrier at 8 GHz is measured using the same dual DO-MZM setup. For this, the optical output power of the MMLL is divided into two using a beam splitter (BS). One part of the light is used for the microwave generation setup, and the other half served as the optical reference. In this configuration, the laser noise is a common mode and cancels out in the baseband. The remaining noise includes all technical limitations of the setup, including the flicker noise of the MUTC. For calibration, a YIG oscillator with the same carrier power (2 dBm) is used and confirmed against a phase noise measurement with the commercial signal analyzer (Keysight, N9030A PXA).

Funding

Lockheed Martin Corporation.

Acknowledgments

The authors thank Dr. Franklyn Quinlan (NIST), Dr. Scott A. Diddams (NIST), and Dr. Mark Notcutt (Stable Laser Systems) for helpful discussions and equipment loans. We also thank Rich Mirin (NIST) and Kevin Silverman (NIST) for molecular-beam epitaxy growth of the SESAM. Part of this research was financially supported by Lockheed Martin Co.

Disclosures

The authors declare no competing interests.

Optics EXPRESS

References

1. P. Ghelfi, F. Laghezza, F. Scotti, G. Serafino, A. Capria, S. Pinna, D. Onori, C. Porzi, M. Scaffardi, A. Malacarne, V. Vercesi, E. Lazzeri, F. Berizzi, and A. Bogoni, "A fully photonics-based coherent radar system," Nature **507**(7492), 341–345 (2014).
2. S. Koenig, D. Lopez-Diaz, J. Antes, F. Boes, R. Henneberger, A. Leuther, A. Tessmann, R. Schmogrow, D. Hillerkuss, R. Palmer, T. Zwick, C. Koos, W. Freude, O. Ambacher, J. Leuthold, and I. Kallfass, "Wireless sub-THz communication system with high data rate," Nat. Photonics **7**(12), 977–981 (2013).
3. J. Millo, M. Abgrall, M. Lours, E. M. L. English, H. Jiang, J. Gúna, A. Clairon, M. E. Tobar, S. Bize, Y. Le Coq, and G. Santarelli, "Ultralow noise microwave generation with fiber-based optical frequency comb and application to atomic fountain clock," Appl. Phys. Lett. **94**(14), 141105 (2009).
4. G. C. Valley, "Photonic analog-to-digital converters," Opt. Express **15**(5), 1955–1982 (2007).
5. E. N. Ivanov and M. E. Tobar, "Low phase-noise sapphire crystal microwave oscillators: current status," IEEE Trans. Sonics Ultrason. **56**(2), 263–269 (2009).
6. E. N. Ivanov and M. E. Tobar, "Low phase-noise microwave oscillators with interferometric signal processing," IEEE Trans. Microwave Theory Tech. **54**(8), 3284–3294 (2006).
7. L. Maleki, "The optoelectronic oscillator," Nat. Photonics **5**(12), 728–730 (2011).
8. J. Li, X. Yi, H. Lee, S. A. Diddams, and K. J. Vahala, "Electro-optical frequency division and stable microwave synthesis," Science **345**(6194), 309–313 (2014).
9. J. Liu, E. Lucas, A. S. Raja, J. He, J. Riemensberger, R. N. Wang, M. Karpov, H. Guo, R. Bouchand, and T. J. Kippenberg, "Photonic microwave generation in the X- and K-band using integrated soliton microcombs," Nat. Photonics **14**(8), 486–491 (2020).
10. G. J. Schneider, J. A. Murakowski, C. A. Schuetz, S. Shi, and D. W. Prather, "Radiofrequency signal-generation system with over seven octaves of continuous tuning," Nat. Photonics **7**(2), 118–122 (2013).
11. J. Li, X. Yi, H. Lee, S. A. Diddams, and K. J. Vahala, "Electro-optical frequency division and stable microwave synthesis," Science **345**(6194), 309–313 (2014).
12. P. Brochard, S. Schilt, and T. Südmeyer, "Ultra-low noise microwave generation with a free-running optical frequency comb transfer oscillator," Opt. Lett. **43**(19), 4651–4654 (2018).
13. W. Liang, D. Eliyahu, V. S. Ilchenko, A. A. Savchenkov, A. B. Matsko, D. Seidel, and L. Maleki, "High spectral purity Kerr frequency comb radio frequency photonic oscillator," Nat. Commun. **6**(1), 7957 (2015).
14. T. M. Fortier, M. S. Kirchner, F. Quinlan, J. Taylor, J. C. Bergquist, T. Rosenband, N. Lemke, A. Ludlow, Y. Jiang, C. W. Oates, and S. A. Diddams, "Generation of ultrastable microwaves via optical frequency division," Nat. Photonics **5**(7), 425–429 (2011).
15. X. Xie, R. Bouchand, D. Nicolodi, M. Giunta, W. Hansel, M. Lezius, A. Joshi, S. Datta, C. Alexandre, M. Lours, P. A. Tremblin, G. Santarelli, R. Holzwarth, and Y. L. Coq, "Photonic microwave signals with zeptosecond-level absolute timing noise," Nat. Photonics **11**(1), 44–47 (2017).
16. T. Nakamura, J. Davila-Rodriguez, H. Leopardi, J. A. Sherman, T. M. Fortier, X. Xie, J. C. Campbell, W. F. McGrew, X. Zhang, Y. S. Hassan, D. Nicolodi, K. Beloy, A. D. Ludlow, S. A. Diddams, and F. Quinlan, "Coherent optical clock down-conversion for microwave frequencies with $10^{(18}$ instability," Science **368**(6493), 889–892 (2020).
17. D. Nicolodi, B. Argence, W. Zhang, R. Le Targat, G. Santarelli, and Y. Le Coq, "Spectral purity transfer between optical wavelengths at the 10−18 level," Nat. Photonics **8**(3), 219–223 (2014).
18. T. D. Shoji, W. Xie, K. L. Silverman, A. Feldman, T. Harvey, R. P. Mirin, and T. R. Schibli, "Ultra-low-noise monolithic mode-locked solid-state laser," Optica **3**(9), 995–998 (2016).
19. M. Endo, T. D. Shoji, and T. R. Schibli, "Ultralow noise optical frequency combs," IEEE J. Sel. Top. Quantum Electron. **24**(5), 1–13 (2018).
20. K. Jung, J. Shin, and J. Kim, "Ultralow phase noise microwave generation from mode-locked Er-fiber lasers with subfemtosecond integrated timing jitter," IEEE Photonics J. **5**(3), 5500906 (2013).
21. A. Beling, X. Xie, and J. C. Campbell, "High-power, high-linearity photodiodes," Optica **3**(3), 328–338 (2016).
22. S. A. Diddams, M. Kirchner, T. Fortier, D. Braje, A. M. Weiner, and L. Hollberg, "Improved signal-to-noise ratio of 10 GHz microwave signals generated with a mode-filtered femtosecond laser frequency comb," Opt. Express **17**(5), 3331–3340 (2009).
23. H. Jiang, J. Taylor, F. Quinlan, T. Fortier, and S. A. Diddams, "Noise floor reduction of an Er:Fiber laser-based photonic microwave generator," IEEE Photonics J. **3**(6), 1004–1012 (2011).
24. F. Quinlan, F. N. Baynes, T. M. Fortier, Q. Zhou, A. Cross, J. C. Campbell, and S. A. Diddams, "Optical amplification and pulse interleaving for low-noise photonic microwave generation," Opt. Lett. **39**(6), 1581–1584 (2014).
25. W. Zhang, T. Li, M. Lours, S. Seidelin, G. Santarelli, and Y. Le Coq, "Amplitude to phase conversion of InGaAs pin photodiodes for femtosecond lasers microwave signal generation," Appl. Phys. B **106**(2), 301–308 (2012).
26. Z. Li, H. Pan, H. Chen, A. Beling, and J. C. Campbell, "high-saturation-current modified uni-traveling-carrier photodiode with cliff layer," IEEE J. Quantum Electron. **46**(5), 626–632 (2010).
27. M. Endo, T. D. Shoji, and T. R. Schibli, "High-sensitivity optical to microwave comparison with dual-output Mach-Zehnder modulators," Sci. Rep. **8**(1), 4388 (2018).
28. A. Hati, C. W. Nelson, D. P. Pappas, and D. A. Howe, "Phase noise measurements with a cryogenic power-splitter to minimize the cross-spectral collapse effect," Rev. Sci. Instrum. **88**(11), 114707 (2017).

Optics EXPRESS

29. A. Hati, C. W. Nelson, and D. A. Howe, "Cross-spectrum measurement of thermal-noise limited oscillators," Rev. Sci. Instrum. **87**(3), 034708 (2016).
30. F. Quinlan, T. M. Fortier, H. Jiang, and S. A. Diddams, "Analysis of shot noise in the detection of ultrashort optical pulse trains," J. Opt. Soc. Am. B **30**(6), 1775–1785 (2013).
31. F. Quinlan, T. M. Fortier, H. Jiang, A. Hati, C. Nelson, Y. Fu, J. C. Campbell, and S. A. Diddams, "Exploiting shot noise correlations in the photodetection of ultrashort optical pulse trains," Nat. Photonics **7**(4), 290–293 (2013).
32. Poseidon Scientific Instruments Pty Ltd., A mobile Ultra-low Phase Noise Sapphire Oscillator, https://www.microwavejournal.com/articles/3367-a-mobile-ultra-low-phase-noise-sapphire-oscillator.
33. M. Endo and T. R. Schibli, "Residual phase noise suppression for Pound-Drever-Hall cavity stabilization with an electro-optic modulator," OSA Continuum **1**(1), 116 (2018).
34. W. F. Walls, "Cross-correlation phase noise measurements," in *Proceedings of the 1992 IEEE Frequency Control Symposium* (IEEE, 1992), pp. 257–261.